applied optics

All-optical logic gates based on nonlinear plasmonic ring resonators

Najmeh Nozhat[1,*] and Nosrat Granpayeh[2]

[1]Faculty of Electrical Engineering, Shiraz University of Technology, Shiraz, Iran
[2]Center of Excellence in Electromagnetics, Optical Communication Laboratory, Faculty of Electrical Engineering, K. N. Toosi University of Technology, Tehran, Iran
*Corresponding author: nozhat@sutech.ac.ir

Received 28 May 2015; revised 13 August 2015; accepted 13 August 2015; posted 14 August 2015 (Doc. ID 241873); published 3 September 2015

A nonlinear plasmonic T-shaped switch based on a square-shaped ring resonator is simulated by the finite-difference time-domain numerical method. Three optical logic gates—a NOT, with one T-shaped switch, and AND and NOR gates, each with two cascaded T-shaped switches—are proposed. The nonlinear Kerr effect is utilized to show the performance of our proposed logic gates. The values of transmission at the ON and OFF states of NOT and NOR gates are 70% and less than 0.6% of the input lightwave, respectively, while these values for the AND gate are 90% and less than 30%, respectively. © 2015 Optical Society of America

OCIS codes: (190.3270) Kerr effect; (250.5403) Plasmonics; (250.6715) Switching; (230.3750) Optical logic devices.

http://dx.doi.org/10.1364/AO.54.007944

1. INTRODUCTION

All-optical devices based on surface plasmon polaritons (SPPs) have been the subject of extensive researches in recent years. SPPs confine electromagnetic waves in subwavelength scales; hence, devices based on SPPs are appropriate solutions for overcoming the diffraction limit. SPPs are the interaction of electromagnetic waves and the free electrons of metals, propagating on the metal–dielectric interfaces [1,2]. Various passive and active plasmonic devices, such as nanocavities, multi/demultiplexers, splitters, couplers, resonators, stub waveguides, Bragg reflectors, hybrid plasmonic waveguides, switches, and logic gates, have been investigated so far [3–15].

Nonlinear plasmonic waveguides can be used in optical signal processing, optical communication networks, and optical computing systems, as all-optical switches and logic gates [16,17]. Several effects have been used to achieve all-optical logic gates, such as four wave mixing (FWM) in silicon nanowires [18], semiconductor optical amplifiers [19], two-photon absorption in silicon waveguides [20], and third-order nonlinear effects [21]. Moreover, some logic gates based on SPPs have been investigated [22–27].

Ring resonators have been used for many applications, such as wavelength and mode selection, switching, filtering, wavelength multi/demultiplexing, and electromagnetically induced transparency-like transmission [15,28,29]. Also, ring resonators with nonlinear Kerr effect or other tunable procedures have been employed for design of all-optical logic gates.

Compared to circular ring resonators, rectangular-shaped ones have higher coupling efficiency due to the long coupling section between the bus waveguide and the resonator. Furthermore, contrary to dielectric waveguides, plasmonic bent waveguides can provide higher transmission with lower bending loss [15].

In this paper, we propose three all-optical logic gates based on nonlinear plasmonic square ring resonators (NLPSRRs). Nonlinear self-phase modulation and cross-phase modulation Kerr effects are utilized to control the light in our nanoscale device. The subwavelength size and the low required pumping power of the NLPSRR switch make it suitable for application in photonic integrated circuits.

The paper is organized as follows. In Section 2, the performance of a plasmonic T-shaped switch is studied. In Section 3, the performance of three optical logic gates—a NOT, with a T-shaped switch, and AND and NOR gates, each with two cascaded T-shaped switches—are simulated and their performance is demonstrated. The paper is concluded in Section 4.

2. NONLINEAR PLASMONIC T-SHAPED SWITCH

The schematic view of the plasmonic T-shaped switch is shown in Fig. 1. It consists of a square-shaped ring resonator and two perpendicular straight waveguides adjacent to it. The switch has input ports A and B for the signal and pump lightwaves, respectively. For better performance of the switch in the third telecommunication window, the parameters of the structure are chosen as: waveguide width $w = 50$ nm, waveguide and ring gap $g = 20$ nm, and side length of the square ring in the x and z directions $L = 570$ nm.

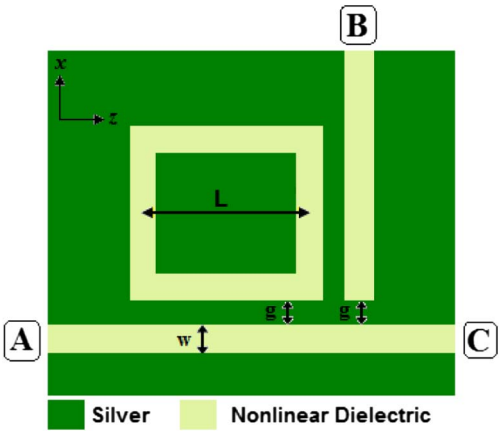

Fig. 1. Schematic view of our proposed nonlinear plasmonic T-shaped switch.

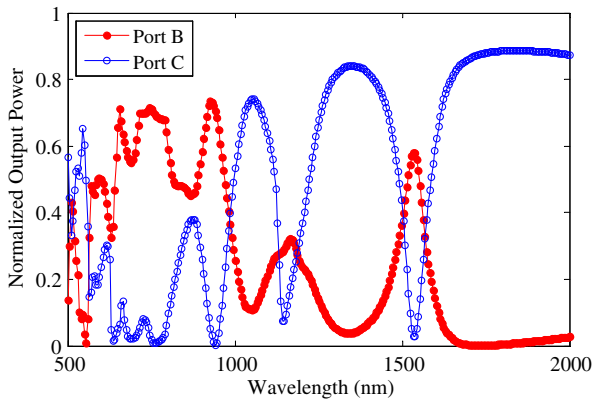

Fig. 2. Transmittance spectra of the plasmonic T-shaped switch of Fig. 1.

The metal and dielectric materials are silver and SiO_2 composite, respectively. The linear refractive index and the third-order nonlinear susceptibility of the dielectric are $n_o = 1.47$ and $\chi^{(3)} = 2.37 \times 10^{-15}$ (m^2/V^2), respectively [14]. The dispersive dielectric function of the silver is described by the Drude model:

$$\varepsilon(\omega) = \varepsilon_\infty - \frac{\omega_p^2}{\omega^2 - j\gamma_p\omega}, \tag{1}$$

where $\varepsilon_\infty = 1.95$ is the relative permittivity at infinite frequency, and $\omega_p = 1.37 \times 10^{16}$ (rad/s) and $\gamma_p = 20 \times 10^{12}$ (rad/s) are the plasma and collision angular frequencies, respectively [12]. The resonant wavelength of the ring resonator is determined by [2]:

$$Ln_{\text{eff}} = m\lambda/4, \tag{2}$$

where m, the mode number, is an integer, and n_{eff} and λ are the ring effective refractive index and the free space wavelength, respectively. According to Eq. (2), the switch is designed for the resonant wavelength of 1535 nm.

The effective refractive index of SPP modes for TM polarization in metal–insulator–metal (MIM) waveguide can be obtained from the dispersion relation [9]:

$$\tanh\left(k_0 d\sqrt{n_{\text{eff}}^2 - \varepsilon_d}\right) = -\frac{\varepsilon_d\sqrt{n_{\text{eff}}^2 - \varepsilon_m}}{\varepsilon_m\sqrt{n_{\text{eff}}^2 - \varepsilon_d}}, \tag{3}$$

where $k_0 = 2\pi/\lambda$ is the free space wave number, and ε_d and ε_m are the dielectric constants of the dielectric and metal, respectively.

The two-dimensional finite-difference time-domain (2D-FDTD) numerical method, with a convolutional perfectly matched layer (CPML) as the absorbing boundary condition of the area under simulation, has been used. Since the width of the waveguide is much smaller than the operating wavelength, only the fundamental TM mode is supported. The output normalized transmission spectra of the switch for an input Gaussian modulated pulse with the power of 9.3×10^{-11} (W/μm) are shown in Fig. 2.

In the linear state with low power input signal, when the wavelength of the input lightwave is equal to the resonant wavelength of the ring, the input lightwave couples to the ring and there is no power at port C, which means that the switch is at the OFF state. In other words, when the wavelength of the input lightwave is out of the resonant wavelength of the ring, there is no coupling to the ring and port C is ON. By launching a high-power input lightwave, due to the Kerr nonlinear effect, the refractive index and so the resonant wavelength of the ring are increased and the status of the switch changes.

The ratio of the powers at ports B and C (P_B/P_C) at the wavelength of 1535 nm is depicted in Fig. 3. The power ratio decreases from 7.1 to −11.7 dB for input powers in the range of 1.98×10^{-8} – 0.0125 (W/μm).

3. ALL-OPTICAL LOGIC GATES

A. NOT Gate

To use the nonlinear T-shaped switch of Fig. 1 as an all-optical NOT logic gate, the switching performance in the simultaneous presence of the bias signal and the input lightwave is studied. A bias signal at the wavelength of 1628 nm and power of 1.99×10^{-8} (W/μm) and an input lightwave at

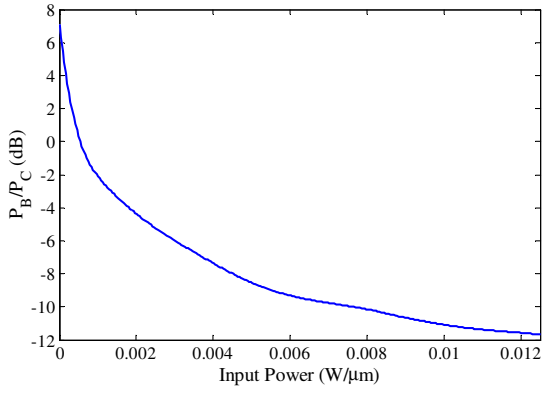

Fig. 3. Power ratio (P_B/P_C) versus input lightwave power for the nonlinear plasmonic T-shaped switch of Fig. 1.

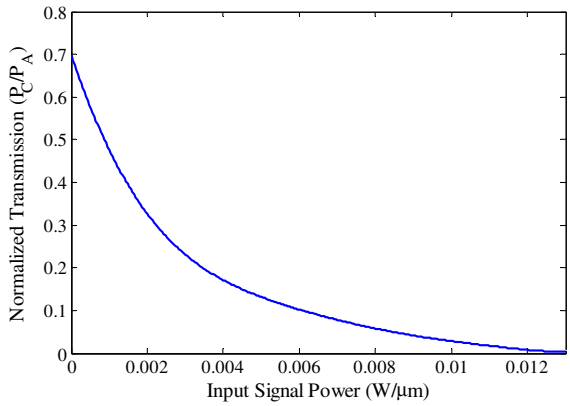

Fig. 4. Normalized transmission diagram of port C versus input lightwave power at port B.

the wavelength of 1535 nm are launched to ports A and B, respectively. The wavelength of the bias signal is chosen to be higher than the resonant wavelength of the ring. As shown in the transmission diagram of Fig. 4, in the linear case, when there is a low level signal with power of 1.51×10^{-8} (W/μm) at port B, the transmission at output port C is 70%, which gives logic 1 (C = B′). In the high-level state with the input power of 0.013 (W/μm), port C is OFF and the transmission is about 0.6%, which corresponds to the logic 0 (C = B′). The magnetic field distributions of the NOT gate in the absence and presence of the input lightwave are illustrated in Fig. 5.

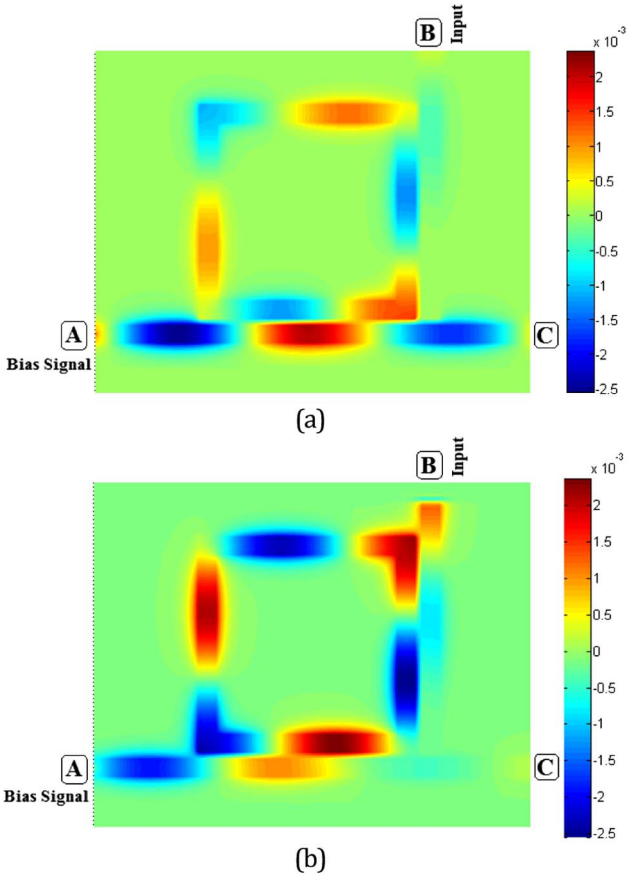

Fig. 5. Magnetic field distributions of the NOT gate in the (a) absence and (b) presence of the input lightwave at wavelength of 1535 nm. Output port C is at ON and OFF states (C = B′), respectively.

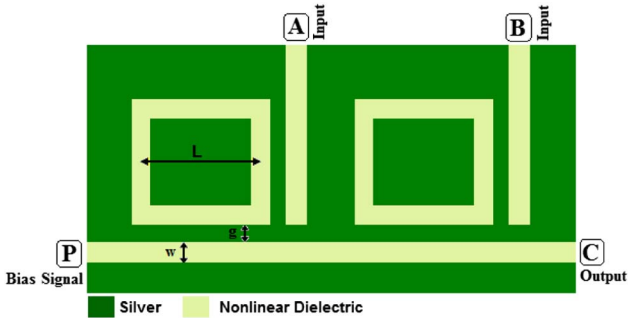

Fig. 6. Schematic view of the plasmonic NOR gate structure.

To obtain the response time of the NOT logic gate, bias and high-intensity continuous wave (CW) pulses at 1628 and 1535 nm wavelengths are, respectively, launched to ports A and B of Fig. 1. By time monitoring of output port C, when the output port approaches the steady state, the switching time is attained to be 11 fs.

B. NOR Gate

An all-optical logic gate can be constructed by cascading two T-shaped switches of Fig. 1, as depicted in Fig. 6. A CW bias signal at wavelength of 1628 nm and two input lightwaves at wavelength of 1535 nm are simultaneously launched to ports P, A, and B, respectively. The distance between the rings is assumed to be 100 nm to avoid crosstalk between them.

According to the performance of the T-shaped switch described in Section 2, the structure of Fig. 6 can act as a NOR gate. When one of the input signals A or B or both of them are ON with power of 0.007 (W/μm), the low-intensity bias signal is coupled to the one or both of the ring resonators and the normalized transmission at port C is less than 0.6%. Therefore, port C is OFF, which gives the logic 0 at the output. However, when both of the input signals A and B are OFF, the bias signal transmits through the bus waveguide. The normalized transmission at output port C is 70%, which would be logic 1. The magnetic field distributions of these states are shown in Fig. 7. The response time of the NOR logic gate is measured by the same method as that described in Subsection 3.A to be 13 fs.

C. AND Gate

The structure of the NOR logic gate of Fig. 6 can also be used as an AND logic gate, if we swap the wavelengths of the bias and input signals. When there is no signal at input ports A and/or B, since the wavelength of the low-intensity bias signal is equal to the resonant wavelength of the ring resonators, it is coupled to the rings, so output port C becomes logic 0. Moreover, when there is a high lightwave with

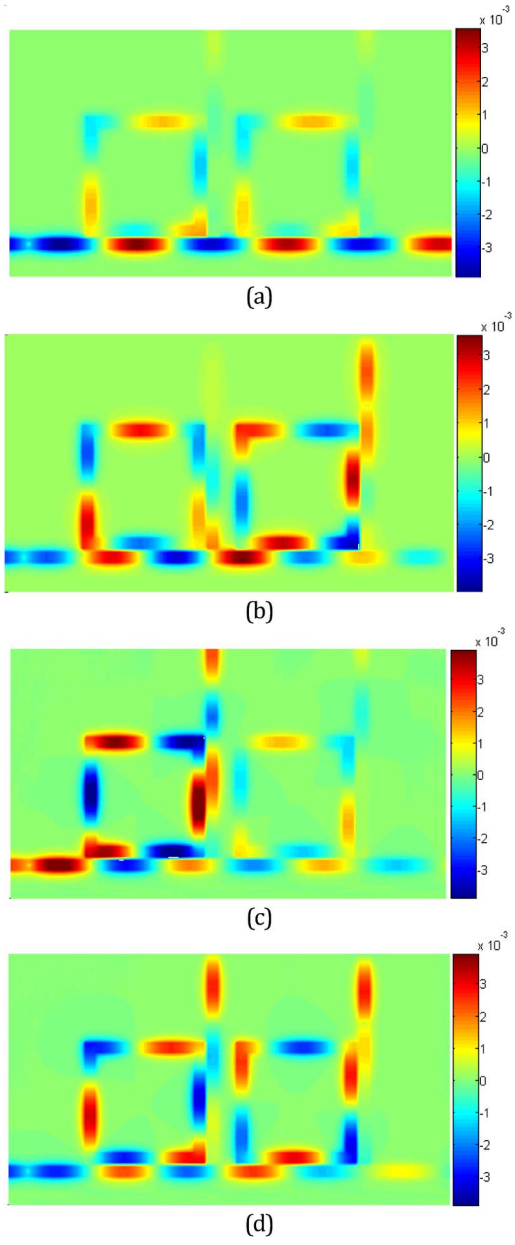

Fig. 7. Magnetic field distributions of our proposed plasmonic NOR gate for four states: (a) both inputs, (b) input A, and (c) input B are 0; and (d) both inputs are 1.

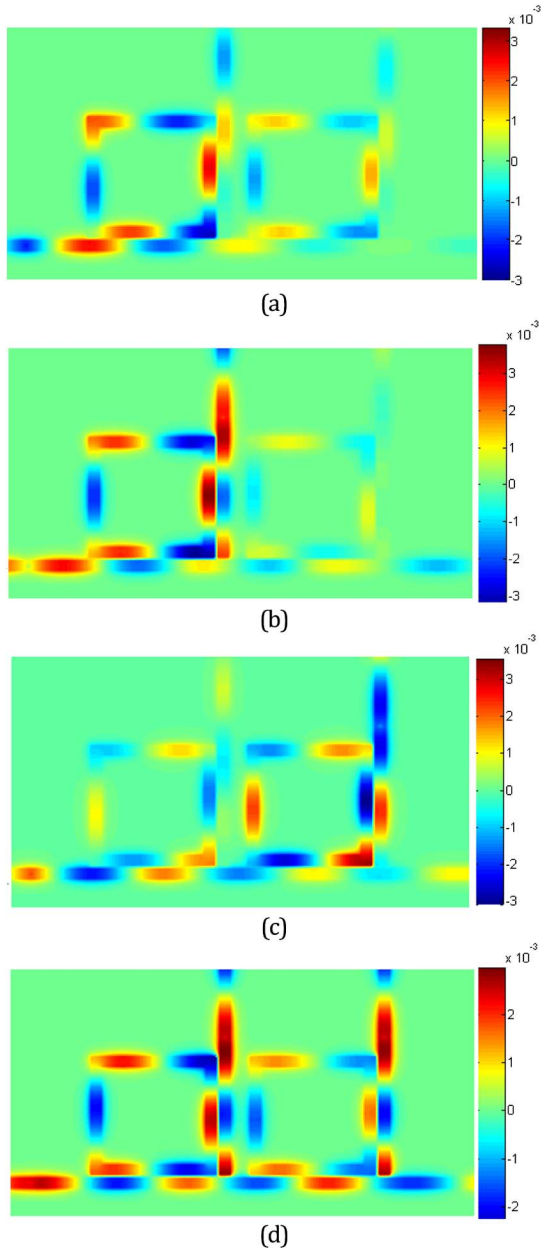

Fig. 8. Magnetic field distributions of our proposed plasmonic AND gate for four states: (a) both inputs, (b) input A, and (c) input B are 0; and (d) both inputs are 1.

power of 0.004 (W/μm) at input ports A or B, the refractive index and so the resonant wavelength of the rings increases, the bias signal is coupled to one of the rings, and there is no power at output port C. Otherwise, when both input ports A and B are ON, because of the enhancement of the resonant wavelength of the rings, the signal transmits through the straight waveguide, hence port C is logic 1. The values of the transmission at the ON and OFF states are 90% and less than 30%, which gives logics 1 and 0, respectively. The magnetic field distributions of these states are shown in Fig. 8. The response time of the AND logic gate is measured by the same method as those of the NOT and NOR gates to be 13 fs.

4. CONCLUSION

In this paper, the performance of a nonlinear plasmonic T-shaped switch based on the nonlinear cross-phase modulation Kerr effect has been demonstrated. We have proposed three all-optical logic gates—NOT, AND, and NOR. The NOT gate is constructed with one T-shaped switch, and the AND and NOR gates are constructed by cascading two T-shaped switches. The transmission of our proposed NOT and NOR logic gates at the ON state is 70%, while at the OFF state it is less than 0.6% of the input power. For the AND gate, the values of transmission at logic 1 and logic 0 are 90% and less than 30%, respectively. Therefore, there is

a high contrast ratio between the ON and OFF states. The subwavelength size and the low required pumping power of the nonlinear plasmonic square ring resonator switch and logic gates with perpendicular waveguides make it suitable for application in photonic integrated circuits.

REFERENCES

1. X. Mei, X. G. Huang, and T. Jin, "A sub-wavelength electro-optic switch based on plasmonic T-shaped waveguide," Plasmonics **6**, 613–618 (2011).
2. X. Peng, H. Li, C. Wu, G. Cao, and Z. Liu, "Research on transmission characteristics of aperture-coupled square-ring resonator based filter," Opt. Commun. **294**, 368–371 (2013).
3. J. Tao, X. G. Huang, X. Lin, Q. Zhang, and X. Jin, "A narrow-band subwavelength plasmonic waveguide filter with asymmetrical multiple-teeth-shaped structure," Opt. Express **17**, 13989–13994 (2009).
4. X. S. Lin and X. G. Huang, "Tooth-shaped plasmonic waveguide filters with nanometeric sizes," Opt. Lett. **33**, 2874–2876 (2008).
5. Y. Guo, L. Yan, W. Pan, B. Luo, K. Wen, Z. Guo, and X. Luo, "Transmission characteristics of the aperture-coupled rectangular resonators based on metal-insulator-metal waveguides," Opt. Commun. **300**, 277–281 (2013).
6. B. Wang and G. P. Wang, "Plasmon Bragg reflectors and nanocavities on flat metallic surfaces," Appl. Phys. Lett. **87**, 013107 (2005).
7. N. Nozhat and N. Granpayeh, "Analysis of the plasmonic power splitter and MUX/DEMUX suitable for photonic integrated circuits," Opt. Commun. **284**, 3449–3455 (2011).
8. J. Chen, Z. Li, M. Lei, X. Fu, J. Xiao, and Q. Gong, "Plasmonic Y-splitters of high wavelength resolution based on strongly coupled-resonator effects," Plasmonics **7**, 441–445 (2012).
9. Z. J. Zhong, Y. Xu, S. Lan, Q. F. Dai, and L. J. Wu, "Sharp and asymmetric transmission response in metal-dielectric-metal plasmonic waveguides containing Kerr nonlinear media," Opt. Express **18**, 79–86 (2010).
10. Y. Bian and Q. Gong, "Optical performance of one-dimensional hybrid metal-insulator-metal structures at telecom wavelength," Opt. Commun. **308**, 30–35 (2013).
11. Y. Bian and Q. Gong, "Low-loss hybrid plasmonic modes guided by metal-coated dielectric wedges for subwavelength light confinement," Appl. Opt. **52**, 5733–5741 (2013).
12. H. Li, J. W. Noh, Y. Chen, and M. Li, "Enhanced optical forces in integrated hybrid plasmonic waveguides," Opt. Express **21**, 11839–11851 (2013).
13. N. Nozhat and N. Granpayeh, "Switching power reduction in the ultra-compact Kerr nonlinear plasmonic directional coupler," Opt. Commun. **285**, 1555–1559 (2012).
14. J. Tao, Q. J. Wang, and X. G. Huang, "All-optical plasmonic switches based on coupled nano-disk cavity structures containing nonlinear material," Plasmonics **6**, 753–759 (2011).
15. N. Nozhat and N. Granpayeh, "All-optical nonlinear plasmonic ring resonator switches," J. Mod. Opt. **61**, 1690–1695 (2014).
16. Y. D. Wu, T. T. Shih, and M. H. Chen, "New all-optical logic gates based on local nonlinear Mach-Zehnder interferometer," Opt. Express **16**, 248–257 (2008).
17. Q. Li and H. Yuan, "All-optical logic gates based on cross-phase modulation in an asymmetric coupler," Opt. Commun. **319**, 90–94 (2014).
18. F. Li, T. D. Vo, C. Husko, M. Pelusi, D. X. Xu, A. Densmore, R. Ma, S. Janz, B. J. Eggleton, and D. J. Moss, "All-optical XOR logic gate for 40 Gb/s DPSK signals via FWM in a silicon nanowire," Opt. Express **19**, 20364–20371 (2011).
19. S. Kaur and R. S. Kaler, "Ultrahigh speed reconfigurable logic operations based on single semiconductor optical amplifier," J. Opt. Soc. Korea **16**, 13–16 (2012).
20. T. K. Liang, L. R. Numes, M. Tsuchiya, K. S. Abedin, T. Miyazaki, D. V. Thourhout, W. Bogaetrs, P. Dumon, R. Baets, and H. K. Tsang, "High speed logic gate using two-photon absorption in silicon waveguides," Opt. Commun. **265**, 171–174 (2006).
21. Y. Liu, F. Qin, Z. M. Meng, F. Zhou, Q. H. Mao, and Z. Y. Li, "All-optical logic gates based on two-dimensional low-refractive-index nonlinear photonic crystal slabs," Opt. Express **19**, 1945–1953 (2011).
22. A. Dolatabady and N. Granpayeh, "All optical logic gates based on two dimensional plasmonic waveguides with nanodisk resonators," J. Opt. Soc. Korea **16**, 432–442 (2012).
23. D. Pan, H. Wei, and H. Xu, "Optical interferometric logic gates based on metal slot waveguide network realizing whole fundamental logic operations," Opt. Express **21**, 9556–9562 (2013).
24. L. Wang, L. Yan, Y. Guo, K. Wen, W. Pan, and B. Luo, "Optical quasi logic gates based on polarization-dependent four-wave mixing in subwavelength metallic waveguides," Opt. Express **21**, 14442–14451 (2013).
25. Y. Bian and Q. Gong, "Compact all-optical interferometric logic gates based on one-dimensional metal-insulator-metal structures," Opt. Commun. **313**, 27–35 (2014).
26. K. J. A. Ooi, H. S. Chu, P. Bai, and L. K. Ang, "Electro-optical graphene plasmonic logic gates," Opt. Lett. **39**, 1629–1632 (2014).
27. I. S. Maksymov, "Optical switching and logic gates with hybrid plasmonic-photonic crystal nanobeam cavities," Phys. Lett. A **375**, 918–921 (2011).
28. K. Wen, L. Yan, W. Pan, B. Luo, Z. Guo, Y. Guo, and X. Luo, "Electromagnetically induced transparency-like transmission in a compact side-coupled T-shaped resonator," J. Lightwave Technol. **32**, 1701–1707 (2014).
29. S. I. Bozhevolnyi, V. S. Volkov, E. Devaux, J. Y. Laluet, and T. W. Ebbesen, "Channel plasmon subwavelength waveguide components including interferometers and ring resonators," Nature **440**, 508–511 (2006).